Modeling the kinetics of light cuts catalytic cracking
Development of a predictive tool

T. Porfírio Fonseca[1]; J. Fernandes[2]; C.I.C. Pinheiro[1]

[1]*Instituto Superior Técnico, University of Lisbon, Av. Rovisco Pais, 1049-0901 Lisbon, Portugal*
[2]*IFP Energies Nouvelles, Rond-point de l'échangeur de Solaize, BP 3, 69360 Solaize, France*

Abstract

The propylene demand is quickly increasing. This product is an important intermediary for the production of several petrochemical derivatives such as polypropylene. For that reason the research for new techniques and on-purpose routes to produce propylene are rising. FCC units produce propylene as a by-product. To achieve the market demand in terms of propylene has been proposed the creation of different upgrades on FCC. One of them consists in adding a second riser which is fed with light stream coming from the main riser or from other refinery units. With this configuration is possible to improve the propylene to over 12%. To predict the yields for each type of feedstock, IFPEN is developing a simulator capable to predict the kinetic performance. The previous version of this simulator estimates with accuracy the yields for PONA composition. The model is shaped for catalytic gasoline and oligomer feeds with different sets of parameters.The aim of the present work is the improvement of this predictive tool, by including isoparaffins, and also the estimation of a set of parameters for coker gasoline. For that, new components were considered and also the reactions involving isoparaffins: catalytic and thermal cracking and isomerization. Its implementation increased the execution time five to eleven times. It was possible to group in one set the parameters for gasolines. The oligomers are described in different sets of parameters. Globally, it was not achieved better results comparing to 2012 data, but the first approach to introduce the new family was successfully accomplished.

Keywords: propylene, fluid catalytic cracking, modeling, kinetics, second riser, isoparaffins

1. Introduction

The propylene is an important intermediary for the production of petrochemicals such as polypropylene, propylene oxide and cumene. The propylene production is achieved mainly by non-catalytic steam cracking of natural gas liquids, naphtha, or gas oil naphtha [1]. Generally, the steam cracking objective is to increase the ethylene production. When using naphtha as the feedstock, the process usually gives an ethylene/propylene ratio of 2:1 [1]. Moreover, the abundance of shale gas has caused gas price to decrease relatively to oil price. Therefore, the cracker operators are driven to use more ethane instead of heavier feeds, which are more expansive. However, the use of ethane as steam cracker feedstock produces less propylene and consequently the propylene price has risen. With propylene demand growing faster than ethylene, combined with the building of more ethane crackers rather than naphtha crackers, the research of new techniques and on-purpose routes are rising [2].

The Fluidized Catalytic Cracking (FCC) process is not an on-purpose process to produce propylene, however it represents the second biggest contributor for propylene production as by product.

Besides, the FCC is a highly adaptable conversion process enabling to adjust propylene/gasoline/diesel production according to market demand [3]. Therefore, concerning the demand increase in diesel and the corresponding decrease of gasoline, and also the demand increase of propylene, the FCC process has been the object of several studies for maximizing the propylene production [4]. This can be achieved with the conventional FCC with high severity operation and optimal ZSM-5 content in catalyst, leading to propylene yields of 8 to 13% depending on the FCC feed. In addition to the use of ZSM-5 to boost propylene production, other ways to maximize propylene have been studied. One of them is the dual riser configuration in FCC, which is studied in the present work.

In the dual riser configuration a second riser is added to the conventional FFC system. This second riser is dedicated to the cracking of a naphtha boiling range type of feed coming from the main riser or from another source available in the refinery. The propylene yield attained with this type of configuration depends on both the main and second riser feeds. For example, with residue feed cracked in the main riser and the recycle of light cracked naphtha (LCN) to the second riser the propylene yield can go up to 12 to 15%. If instead of a LCN an oligomer is fed to the second riser propylene production will be even higher.

Since 2008, a simulator is being developed by IFP Energies Nouvelles (IFPEN) to predict the yields and performances in the second riser of a dual riser FCC configuration. A molecular lumping strategy was implemented where the compounds are divided in four families: paraffins, olefins, naphthenes and aromatics. Later on, the reaction network was modified in 2010 and 2012 by adding new reactions to achieve better results. The effect of ZSM-5 percentage was also introduced in the model in 2012 in order to improve the predictions.

The aim of this work is the model improvement for a better description of reaction kinetics. For this purpose the distinction between normal and branched paraffins will be done. For that, it is necessary to modify the reaction network to take into account the new components. Others changes will be also studied, namely the ZSM-5 effect in hydrogen transfer reaction.

2. Dual riser configuration

In order to achieve the market needs in terms of propylene demand, the dual riser configuration in FCC process has been researched and suggested by different licensors. Axens, an IFPEN group company, proposes several technologies which can use this type of configuration. PetroRiser™ is one of them, which is generally associated with a FCC that treats heavy feeds (R2R unit). In this case part of the catalytic gasoline produced in the main riser is recycled to the second riser. Besides PetroRiser™, the second riser configuration can be adopted for other technologies. One case is the integration of the dual riser FCC unit with an oligomerization unit that produces an oligomer feed which is fed to the second riser.

The dual riser FCC configuration is similar to the conventional FCC process. As suggested by its name, this technology considers two risers: one riser orientated towards conversion of the main feed (the conventional) and another one which is dedicated to the production of propylene by cracking a naphtha boiling type of feed (approximately 30-220°C).

The catalyst cycle is the same for both risers, i.e. the second riser uses the same catalyst and regeneration section. Like for the main riser, in the second riser the catalyst and products are separated by a cyclone. The separated catalyst and products are sent to the stripping and fraction zone respectively (the same than for the main riser).

As referred above, the second riser can have different types of feeds. Recycling the fractions produced in the first riser is normally the first option to improve the propylene production. It is the case of light cracked naphtha (LCN), which is produced in the first riser and separated in the main fractionator and naphtha splitter. After these separations, LCN is recycled to the second riser. Besides catalytic cracked naphtha from FCC, the naphtha sent to the second riser can also have other sources, such as cokers and hydrocrackers units. In addition to the cracked naphthas, it is also possible to use other feed types, such as an oligomer (feed with very high content of olefins). The association of an oligomerization unit to the second riser increases significantly the propylene yields. The integration of the oligomerization unit with the FCC consists in sending the C_4 cut obtained in the FCC main riser to this unit, upgrading this it into a high olefinic stream. Besides the C4 cut, the C_3/C_4 cut can also be fed to this alkylation process.

The FCC converts heavy feeds in lighter and more valuable products. These products are then separated in cuts by their boiling point: dry gas (P_1+P_2+ H_2+H_2S), LPG (P_3, O_3, P_4, O_4), gasoline (C_5-220ºC), LCO (220ºC-360ºC), HCO (360ºC-440ºC) and coke. Since the feed to the second riser is in the gasoline boiling range the products coming out from the second riser are mainly light gases (dry gas and LPG) and gasoline. However, small quantities of heavier products (LCO) and coke are also produced.

The operating conditions for the first riser are typically the same that in the conventional FCC process. On the other hand, the operating conditions for the second riser are more severe than in the first riser [5].

The catalyst is the conventional FCC catalyst composed by the Y zeolite, a matrix and additives such as ZSM-5, metal traps and bottoms-cracking additives. The ZSM-5 is also an important additive that acts as co-catalyst. It is used to improve the octane number of gasoline, the primary product target in conventional FCC process. It is used also to improve the production of light olefins, especially propylene. These improvements are obtained mainly by decreasing the average molecular weight of the gasoline, in particular by cracking most of the long paraffins and olefins (C_{7+}) to produce short paraffins and olefins and by increasing the iso/normal ratio of the paraffins and olefins from C_4 to C_7 [6].

3. Experimental data

The data used in this work was obtained with different naphtha feedstocks and conditions. As referred above, the feed sent to the second riser can have different origins. Concerning the different possibilities, four feeds were tested: catalytic gasoline obtained in a main riser; coker gasoline from a coker process unit; oligomeric feed from an oligomerization unit which is fed by C_3 and C_4 cuts (referred in this work as PolyC3C4); oligomeric feed from an oligomerization unit fed with a C_4 cut (referred as PolyC4).

The detailed composition of the feedstocks was previously obtained by gas chromatography analysis. The oligomeric feeds (PolyC3C4 and PolyC4) are composed mainly by olefins (Fig. 1). The gasolines' composition has a pattern of all the families where the isoparaffins characterizes more than 10% of the feeds. It is also important to refer the aromatic content of catalytic gasoline which is much higher than in the others feeds (namely in the oligomers).

Two equilibrium catalysts (E-cat) were used in the experimental tests: E-cat A in catalytic and coker gasoline and PolyC3C4; and E-cat B in PolyC4 tests.

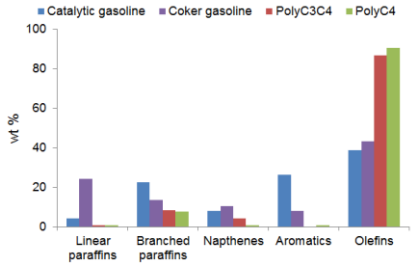

Fig. 1 - Feedstocks PIONA composition in mass percentage

Further comparative characterization of the two catalysts is given in Table 1. The ratio between the values for a given property of the A and B catalyst are presented below.

Table 1 - Properties values ratio between E-cat A and B

Property	A/B catalysts ratio
Z/M ratio	4.1
REO content	2
Ni content	111.3
V content	17.7

Generally, a catalyst with a high content of matrix is well adapted to large molecule cracking of heavy feeds. That is the case of E-cat B that has a higher content of matrix than E-cat A.

The experimental results show that the propylene yield is lower for the gasoline feeds and its highest value was obtained with PolyC4 feed. Moreover, it was observed that all the four feeds produce similar quantities of dry gas and coke yields.

4. Second riser model and simulator

The second riser model, which name is Petroriser, has been developed in IPFEN and is implemented in *Fortran* language.

Sub-chapters 4.1 to 4.4 describe the state of the art where are presented the reactive species, the reactions and main assumptions. Then in sub-chapter 4.5 the proposed modifications to the code are presented. Finally, in sub-chapter 4.6 the optimization procedure is explained.

4.1. Reactive species

The reactive species were lumped according to their chemical nature: paraffins, olefins, naphthenes and aromatics. The lumps considered in the model are the following ones: Paraffins lump (P) concerns the paraffins (linear and branched) with one to twelve carbon atoms; Olefins lump (O) includes the olefins (linear and branched) with two to twelve carbons; Naphthenes lump (N) distinguishes the more reactive naphthenes such as N_6, N_7 and N_8 from the N_{comp} (which groups N_5 and N_{9+}); Aromatics lump (A) includes A_6 to A_{12}; Coke; LCO; H_2; hydrogen hydride, H_2^*. Sulfur and nitrogen compounds are not considered in the model. The kinetic model for the second riser considers then a total of 45 species.

4.2. Reaction network

Firstly, the reaction network was established based on the experimental data described above. Then, the first model version of 2008 implemented by F. Feugnet was upgraded in 2010 and 2012 by adding new reactions and by improving the description of the reaction scheme and catalyst effects.

At present, the reaction network is composed by the following reactions: catalytic cracking (β-scission and protolytic cracking); hydrogen transfer; oligomerization; LCO formation; coke formation; thermal cracking; olefins cyclisation.

Each reaction has different assumptions which are briefly described in the next topics.

Catalytic cracking (β-scission and protolytic cracking)

The catalytic cracking concerns the paraffins and olefins.

The paraffins' cracking mechanism depends of the acid site type where the molecule is absorbed: if it is a Brönsted or a Lewis site. In a Brönsted site, the cracking occurs through

protolytic cracking. If absorbed on a Lewis acid site, the cracking will go through a β-scission mechanism. Nevertheless, in both cracking mechanisms the paraffin absorbed produces a lighter paraffin and an olefin [7]. In this reaction type, it was assumed that just paraffins with more than 5 carbon atoms (P_{5+}) will crack.

On the other hand, the olefins are absorbed by Brönsted acid site and consequently the cracking occurs by β-scission mechanism [7]. In this reaction, the products are only olefins and not an olefin and a paraffin as in the case of paraffins' cracking reaction. For the olefins species cracking is only available for molecules with more than 6 carbon atoms (O_{6+}).

Hydrogen transfer

In the FCC process hydrogen transfer reactions are usually represented between olefins and naphthenes to produce aromatics and paraffins. However, this reaction is commonly referred in the literature for conventional feeds, i.e. heavy feedstocks. For lighter feeds this assumption does not make sense. Experimental data of pure olefins and paraffins cracking shows the occurrence of this reaction without the presence of naphthenes [7]. For this reason, another mechanism is proposed to take into account the olefin cyclisation to produce aromatics. This mechanism is divided in three steps:

- Step 1: Reaction of two olefins to produce an aromatic and three hydrides;
- Step 2: Naphthenes dehydrogenation to produce an aromatic and three hydrides;
- Step 3: Reaction of an olefin and the hydrides from Step 1 and 2 to form a paraffin.

Oligomerization

This reaction was introduced in 2012 to improve the olefins O_3-O_5 fit [8]. The oligomerization reaction promotes C-C bonds formation and occurs with reduction in the number of molecules, so it is thermodynamically favored at low temperature and high pressure.

LCO formation

As assumption, LCO was considered as a di-aromatic molecule which molecular representation is C_xH_y. The LCO is produced from aromatic condensation.

Coke formation

As for the LCO cut, an assumption has to be made for the coke molecular structure. Typically, the coke has 5% in hydrogen [7]. The coke molecular structure will be represented as C_xH_y. Coke is produced from aromatic condensation.

Thermal cracking

Thermal cracking can be divided in two main reactions:

- C-C boundary break:

$$C_{m+n}H_{2(m+n)+2} \rightarrow C_mH_{2m} + C_nH_{2n+2} \quad (1)$$

In this reaction, one paraffin and one olefin are produced. This reaction is a radical reaction which involves a β-scission.

- Dehydrogenation:

$$C_mH_{2m+2} \rightarrow C_mH_{2m} + H_2 \quad (2)$$

Dehydrogenation leads to the formation of H_2. This specie is not, however, observed in experimental data.

Besides the dehydrogenation reaction only happens at 700°C, while the C-C boundary break reaction occurs at temperatures above 300°C. Therefore, the C-C boundary break was considered as the main thermal cracking reaction since in the second riser the temperature (ranges from 580°C to 610°C) does not achieve such high temperature in order that dehydrogenation reactions can take place [7].

It was also assumed that the aromatics and naphthenes do not undergo thermal cracking, and only olefins and paraffins are concerned by this type of reaction. Based on experimental data it was concluded that sensitivity of olefins and paraffins for thermal cracking is different. Therefore, it was considered two sets of reaction to considered separately the olefin and paraffin thermal cracking.

Olefin cyclisation

Olefins cyclisation reactions have been included in the model reaction network in its last version dating from 2012. The objective was to reduce the deviation on aromatics lump. The hydrogen transfer reaction, that produced aromatics, takes places after the cyclisation. Therefore, it was considered the formation of naphthenes from olefin cyclisation. With this assumption the naphthenes formed in this reaction will be considered in hydrogen transfer reaction to form aromatics [9].

The chemical equations of the reaction network are summarized in Table 2 as well as the range of applicability. In these conditions, the reaction network includes 125 reactions.

4.3. Kinetic model

To model the reaction network the kinetic rates for each one of the reactions are given by an Arrhenius law type equation. To simplify the model and due to the lack of experimental data several assumptions were made.

One of the assumptions of this model is that the catalyst deactivation is not taken into account. The coke concentration on catalyst produced from light feeds is normally less than 0.2% even when the reaction finishes, the catalyst decay is, therefore, neglected [10]. Furthermore, the mechanisms of adsorption/desorption are also neglected since it would be difficult to estimate adsorption/desorption rates with the experimental data available. Finally, in order to reduce the number of parameters to estimate, simple expressions relating the rate constant with the nature of the reacting species, their chain length and symmetry have been implemented.

The equations of kinetic rate constant are summarized in Table 2. In the follow paragraphs, the expressions will be described briefly.

In paraffins and olefins catalytic cracking, the kinetic constants are correlated to reactive species chain length like in the model proposed by Carabineiro, et. al (2003) and Pinheiro, et al. (1999). The K^0_{pcr} and K^0_{ocr} are the parameters for the cracking rate magnitude of paraffin and olefins cracking, respectively. These parameters are related to the overall rate of cracking for all the possible reactants of each reaction set. i and j are number of carbon atoms of the reactant and the product, respectively according to the chemical reaction.

By taking into account the reactant chain length and the symmetrical scission in kinetic constant rate calculation, it is possible to use one single rate expression for all reactants [11]. For this, two structure parameters are needed: α_{cr} is the chain-length parameter which is related to the way that cracking rate increases with the number of carbon atoms in the reactant; β_{cr} is the symmetry parameter that defines the variation of the rate constant, with the type of products [12]. The structure parameters have the same values for paraffins and olefins.

Concerning this molecule structure function, the cracking rate follows a normal distribution where the maximum is verified for the symmetrical scission. This can be observed in

Fig. 2 for each i. For example, for $i = 12$, a reactant molecule with 12 carbon atoms, a normal distribution is observed during j, where the maximum is established for cracking in two molecules with 6 carbon atoms each.

Table 2 – State of the art: reaction network and kinetic expressions

Reaction type	Chemical reaction	Kinetic rate constant equation
Paraffins catalytic cracking	$P_i \rightarrow P_j + O_{i-j}$ $5 \le i \le 12$ $3 \le j \le i-3$	$K_{pcr} = K^0_{pcr} \cdot \exp\left(-\frac{Ea_{pcr}}{R}\cdot\left(\frac{1}{T}-\frac{1}{T_{ref}}\right)\right) \cdot \exp\left(-\left(\frac{\alpha_{cr}}{i}+\beta_{cr}\cdot\left(j-\frac{i}{2}\right)^2\right)\right)\left(1+f_{ZSM-5,pcr}(i,j)\right)$
Olefins catalytic cracking	$O_i \rightarrow O_j + O_{i-j}$ $6 \le i \le 12$ $3 \le j \le i-3$	$K_{ocr} = K^0_{ocr} \cdot \exp\left(-\frac{Ea_{ocr}}{R}\cdot\left(\frac{1}{T}-\frac{1}{T_{ref}}\right)\right) \cdot \exp\left(-\left(\frac{\alpha_{cr}}{i}+\beta_{cr}\cdot\left(j-\frac{i}{2}\right)^2\right)\right)\left(1+f_{ZSM-5,ocr}(i,j)\right)$
Hydrogen transfer: step 1	$O_i + O_j \rightarrow A_{i+j} + 3H_2^*$ $2 \le i \le 5$ $3 \le j \le 5$ $i+j \ge 6$	$K_{ht1} = K^0_{ht1} \cdot f_{ht1}(i,j) \cdot (1 + f_{ZSM-5,ht1})$
Hydrogen transfer: step 2	$N_i \rightarrow A_i + 3H_2^*$ $6 \le i \le 8$	$K_{ht2} = K^0_{ht2} \cdot f_{ht2}(i)$
Hydrogen transfer: step 3	$O_i + H_2^* \rightarrow P_i$ $2 \le i \le 12$	$K_{ht3} = K^0_{ht3} \cdot f_{ht3}(i)$
Oligomerization	$O_n + O_i \rightarrow O_{n+i}$ $3 \le n \le 5$ $4 \le i \le 5$	$K_{Oligom,i} = K^0_{Oligom,i} \cdot \exp\left(-\frac{Ea_{Oligom}}{R}\cdot\left(\frac{1}{T}-\frac{1}{T_{ref}}\right)\right)$
LCO formation	$\frac{x_{LCO}}{n}A_n \rightarrow LCO + \frac{1}{2}\times\frac{x_{LCO}(2n-6)-y_{LCO}n}{n}H_2$	$K_{LCO} = K^0_{LCO} \cdot \exp\left(-\frac{Ea_{LCO}}{R}\cdot\left(\frac{1}{T}-\frac{1}{T_{ref}}\right)\right)$
Coke formation	$\frac{x_{Coke}}{n}A_n \rightarrow Coke + \frac{1}{2}\times\frac{x_{Coke}(2n-6)-y_{Coke}n}{n}H_2$	$K_{Coke} = K^0_{Coke} \cdot \exp\left(-\frac{Ea_{Coke}}{R}\cdot\left(\frac{1}{T}-\frac{1}{T_{ref}}\right)\right)$
Paraffins thermal cracking	$O_i \rightarrow O_2 + O_{i-2}$ $4 \le i \le 12$	$K_{th1} = K^0_{th1} \cdot \exp\left(-\frac{Ea_{th1}}{R}\cdot\left(\frac{1}{T}-\frac{1}{T_{ref}}\right)\right) \cdot f_{th1}(i)$
Olefins thermal cracking	$P_j \rightarrow P_1 + O_{j-1}$ $P_j \rightarrow O_2 + P_{j-2}$ $3 \le j \le 12$	$K_{th2} = K^0_{th2} \cdot \exp\left(-\frac{Ea_{th2}}{R}\cdot\left(\frac{1}{T}-\frac{1}{T_{ref}}\right)\right) \cdot f_{th2}(i)$
Olefin cyclisation	$O_i \rightarrow N_i$ $6 \le i \le 8$	$K_{Cycli} = K^0_{Cycli} \cdot \exp\left(-\frac{Ea_{Cycli}}{R}\cdot\left(\frac{1}{T}-\frac{1}{T_{ref}}\right)\right)$

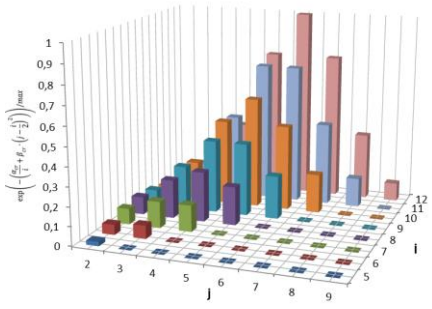

Fig. 2 - Representation of molecule structure function for catalytic cracking normalized with its maximum value

As discussed before, the presence of ZSM-5 promotes the cracking for long paraffins and olefins. This effect was not considered until 2012. At the time, it was introduced a function in order to modulate the kinetic rate increasing in catalytic cracking reactions due to the presence of this zeolite. The influence of ZSM-5 is only considered in the cracking of paraffins from P_7 to P_9 and olefins from O_6 to O_{10} [9]. Fig. 3 describes the function $f_{ZSM-5,cr}$ which has the same behavior for paraffins and olefins cracking. As expected, the function depends of ZSM-5 percentage in the catalyst and its value without ZSM-5 is zero. This function also depends of the number of carbon atoms of the reactant, i. However the variation with carbon number is very limited, i.e. the function is quite similar for all reactions in the same set (olefins or paraffins).

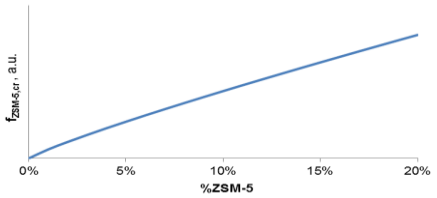

Fig. 3 - ZSM-5 influence for kinetic rate of paraffins and olefins catalytic cracking in function of ZSM-5 content percentage

As described in the previous chapter, the hydrogen transfer reaction is subdivided in three steps. Therefore, the kinetic rate is defined separately for each step. For all of them, it is not considered the activation energy because it was assumed that hydrogen transfer are very fast reactions and therefore independent of temperature level [7]. The function f_{ht1} in kinetic expression takes into account the cracking dependence factor on the reactant carbon chain length similarly to what has been done in Carabineiro's (2003) study. The ZSM-5 does not impacts directly hydrogen transfer reactions, it has been considered that the presence of ZSM-5 in the catalyst has a dilution effect in hydrogen transfer reactions. The zeolites as ZSM-5 show relatively low hydrogen transfer values. The function represented in Fig. 4 introduces the effect of dilution considered for the ZSM-5 content [9]. This function was implemented for the interval between 10% and 18% of ZSM-5 additive in the E-cat, since the experimental data at the time (2012) included only percentages of ZSM-5 content in this range. However, below 10% of ZSM-5, this function should not be applied, since the function increases very significantly when the content of ZSM-5 is lower than 5%.

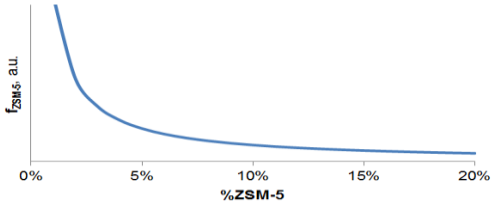

Fig. 4 - ZSM-5 influence for kinetic rate of hydrogen transfer reaction (step 1) in function of ZSM-5 content percentage

4.4. Model implementation

For the model implementation, it is necessary to establish the material and pressure balances. Therefore, it is necessary to make some assumptions: R2R pilot is considered as a plug flow; small pressure drop and consequently the catalyst concentration is uniform along the riser; pressure drop is neglected; isothermal operation (light feeds cracking enthalpy is low).

The material and pressure balances are achieved according to dZ slices as showed in Fig. 5.

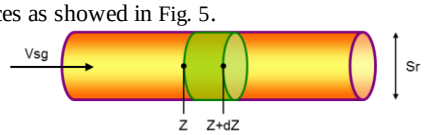

Fig. 5 - Control volume scheme

The several reactions occur in different phases (gas and solid) and depend or not of the presence of the catalyst. Besides there is accumulation of product species in both gas and solid phases. Therefore, the material balances for each phase have to be described separately. First of all, it is essential the distinction between catalytic and thermal reactions. The catalytic reactions take place in the catalyst (solid phase), while the thermal reactions occur in the gas phase. Second, although there are several reactions taking place in the solid phase most of the product species after their formation will desorb from the catalyst and go to the gas phase, except for coke that will remain in the solid phase adsorbed and/or trapped in the catalyst sites leading to catalyst deactivation.

Material balance in gas phase (for catalytic and thermal reactions)

$$(1-\varepsilon_S)\cdot\frac{\partial C_i^g}{\partial t} = -\frac{\partial}{\partial Z}\left(V_{sg}\cdot C_i^g\right) + \rho_S\cdot\varepsilon_S \cdot \sum_{n=1}^{gas\ catalytic\ reactions}(\mu_{i,n}\cdot V_n) + (1-\varepsilon_S)\cdot\sum_{n=1}^{thermal\ reactions}(\mu_{i,n}\cdot V_n') \quad (3)$$

Where: ε_S is the solid void fractions or hold-up; V_{sg} is the superficial gas velocity $(m\ s^{-1})$; ρ_S is the solid density $(kg\ m^{-3})$; C_i^g is the molar concentration of the specie i in the gas phase $(mol\ m^{-3})$; n is the reaction number; V_n is the reaction n rate $(mol\ s^{-1}\ kg_{catalyst}^{-1})$; V_n' is the reaction n rate in $mol\ s^{-1}\ m^{-3}$; $\mu_{i,n}$ is the stoichiometric coefficient of the specie i in the reaction n; t is time (s).

Material balance in solid phase

$$\varepsilon_S\cdot\frac{\partial C_i^s}{\partial t} = \rho_S\cdot\varepsilon_S\cdot\sum_{n=1}^{solid\ catalytic\ reactions}(\mu_{i,n}\cdot V_n) - \frac{\partial}{\partial Z}\left(V_{sg}\cdot C_i^s\right) \quad (5)$$

Finally, it is important to establish the pressure balance in order to describe the volume expansion. The balance is obtained considering the gases mass balances of all the species.

Pressure balance – partial pressure and volume expansion

$$\frac{\partial V_{sg}}{\partial Z} = \frac{RT}{P_t}\cdot(\rho_S\cdot\varepsilon_S)\cdot\left[\sum_{i}^{species\ gas}\sum_{j=1}^{catalytic\ reactions}(\mu_{i,j}\cdot V_n) + (1-\varepsilon_S)\cdot\sum_{i}^{species\ gas}\sum_{j=1}^{thermal\ reactions}(\mu_{i,j}\cdot V'_n)\right] \quad (6)$$

Rate equations

Concerning the calculation of kinetic rate, it is admitted that reactions are elementary, excluding coke formation which is considered a first order reaction.

Therefore, for the reaction n,

$$\mu_{i,n}\cdot[i] + \mu_{j,n}\cdot[j] \rightarrow product\,(s) \quad (7)$$

The components i and j react according to their stoichiometry coefficient $\mu_{i,n}$ and $\mu_{j,n}$ respectively. The kinetic rate is obtained by (8).

$$V_n = K_X P p_i^{\mu_{i,n}} P p_k^{\mu_{j,n}} \quad (8)$$

4.5. Model modifications

- **ZSM-5 effect review**

As described above in chapter 4.3, the ZSM-5 influence is taken into account in hydrogen transfer reaction as a dilution factor. Nevertheless, the equation that describes this effect was established based on data with 10 and 18% of ZSM-5 content. The present function predicts incoherent values for the range between 0% and 10% of ZSM-5. Some experimental tests of coker gasoline were obtained with 0% and 5% of ZSM-5 in the catalyst. For that reason and for coherence purposes the mathematical form of this function had to be reevaluated. The new function is graphically presented in the graph below.

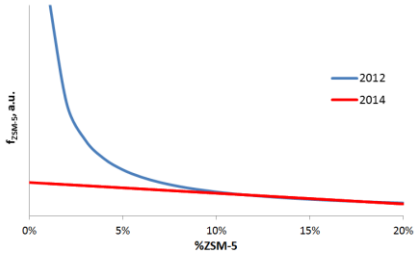

Fig. 6 - Comparison of ZSM-5 effect function in 2012 and its improvement in 2014

In the new approach, it was assumed a smooth decreasing from 0% to 10% and the same behavior in range between 10% and 20%.

LCO formation as a first order reaction

As referred in the model implementation chapter, the reaction to produce LCO is an elementary reaction, meaning that the reaction order for LCO formation is the same as the reactant stoichiometric index for LCO formation which can be relatively high. After reviewing LCO kinetic rate equation, it has been concluded that considering a reaction order dependent on the stoichiometric coefficient was not appropriate for LCO formation. In the new model, LCO formation is therefore considered as a first order reaction. This modification also facilitates the convergence when the reactants leading to LCO formation (Aromatics) are weakly represented, like in the oligomers case.

Isoparaffins implementation

Previous works have taken place at IFPEN with the purpose of improving the second riser model predictions [9]. However, no distinction was made between linear and branched hydrocarbons until now.

Before the isoparaffins implementation in reaction network, it is necessary to make some more assumptions. Starting with the components, the isoparaffins can be mono-branched, di-branched, etc. If it was considered all the types or the majority of possibilities, the number of species and reactions would increase exponentially. Therefore, it was decided to just consider the isoparaffins without the distinction of the number of branches. Consequently, it is necessary to add 9 additional species in the model, representing the isoparaffins with 4 to 12

carbon atoms (iP4 to iP12). The new model will then have a total of 54 molecular lumps.

By splitting paraffins into normal and branched, new reactions need to be implemented in the reaction network. In order to simplify it by reducing the reaction number, it will be assumed:

- The previous reactions or kinetic expressions do not require any changes[1],
- The paraffins and isoparaffins catalytic cracking will only produce linear paraffins,
- The isoparaffins are produced only from isomerization and isoparaffins thermal cracking reactions.

If it had been considered isoparaffins as a product of catalytic cracking, the reaction number would have increased too much for this first approach in implementing isoparaffins in the kinetic model. It was then decided that, for the moment, only the isoparaffins catalytic and thermal cracking and the isomerization reactions would be considered. For the two firsts reactions, the same approach and assumptions for paraffins were made.

The isoparaffins cracking is only present for iP_{5+}, according to the next equation:

$$iP_i \rightarrow P_j + O_{i-j} \tag{9}$$

Where i ranges from 5 to 12 and j from 3 to i-3.

The kinetic rate is defined by (10) which is similar to the one used for paraffin cracking. Nevertheless, the structure parameters are not necessarily the same for normal and branched paraffins. For that reason, it is assumed a different value for these parameters ($\alpha_{cr,iso}$ and $\beta_{cr,iso}$).

$$K_{pcr,iso} = K^0_{pcr,iso} \cdot \exp\left(-\frac{E\,a_{pcr,iso}}{R}\cdot\left(\frac{1}{T}-\frac{1}{T_{ref}}\right)\right) \cdot \exp\left(-\left(\frac{\alpha_{cr,iso}}{i}+\beta_{cr,iso}\cdot\left(j-\frac{i}{2}\right)^2\right)\right) \tag{10}$$

Some studies refer that the pores sizes of ZSM-5 are not enable the access for branched molecules. For this reason, the ZSM-5 effect was not taken into account.

Thermal cracking for isoparaffins was established in the same way that for paraffins. Thermal cracking for branched alkanes is then given according to (11) and (12).

$$iP_j \rightarrow P_1 + O_{j-1} \tag{11}$$

$$iP_j \rightarrow O_2 + iP_{j-2} \tag{12}$$

Where i can have values from 3 to 12.

The kinetic rate constant is defined by (13) in the same way as for paraffin thermal cracking. Once again, the f_{th2} parameters will be different between the both types of paraffins.

$$K_{th2,iso} = K^0_{th2,iso} \cdot \exp\left(-\frac{E\,a_{th2,iso}}{R}\cdot\left(\frac{1}{T}-\frac{1}{T_{ref}}\right)\right)\cdot f_{th2,iso}(i) \tag{13}$$

Differently from the last reactions, the isomerization reaction is a chemical equilibrium between paraffins and isoparaffins (14).

$$P_i \rightleftarrows iP_i \tag{14}$$

Where i ranges between 4 and 12.

In this case, the kinetic rate is more complex than for the previous irreversible reactions. The reversible reaction defines the equilibrium that has to be taken into account in kinetic rate (15).

$$r = K_{i,ISOM}\left(Pp_{nP} - \frac{Pp_{iP}}{K_{eq}}\right) \tag{15}$$

The equilibrium constant is obtained by thermodynamic data which is available in literature [13]. The equilibrium constant, K_{eq} depends of the temperature (16).

$$K_{eq}(T) = \exp\left(-\frac{\Delta G_r(T)}{RT}\right) \tag{16}$$

Where the difference of Gibbs free energy, ΔG_r is given by the equation below.

$$\Delta G_r(T) = \sum_j v_j \Delta H_{f,j}(T) - T\sum_j v_j S_{f,j}(T) \tag{17}$$

With $v_j = 1$ for the isoparaffins and $v_j = -1$ for the paraffins. ΔH_f and S_f are calculated by (18) and (19), respectively.

$$S_f(T) = S°_f + \int_{298}^{t} C_p(T)\,dT \tag{18}$$

$$\Delta H_f(T) = \Delta H°_f + \int_{298}^{t} C_p(T)\,dT \tag{19}$$

The thermodynamic data used in these calculations is from another IFPEN project, and for this reason this data is confidential and will not be presented herein. On the other hand, the kinetic rate constant is obtained using Arrhenius law, where the isomerization constant, K^0_{Isom}, was obtained from parameters estimation for each isomerization reaction (14). The activation energy was considered to be the same for all isomerization reactions.

$$K_{Isom,i} = K^0_{Isom,i} \cdot \exp\left(-\frac{E\,a_{Isom}}{R}\cdot\left(\frac{1}{T}-\frac{1}{T_{ref}}\right)\right) \tag{20}$$

Moreover, the reactions that were introduced were assumed to be elementary reactions.

4.6. Optimization

In the previous sections several parameters have been identified in the kinetic expressions that need to be estimated and optimized. A widely used optimization method is the least squares principle. This method minimizes the sum of the squares of the errors, i.e. of the deviations between the observed values and the values predicted by the model. Hence, the objective function is described by (19).

$$minimize\left\{ssq = \sum_x \left(y_{experimental,x} - y_{calculated,x}\right)^2 W_x\right\} \tag{21}$$

Where W_x represents the weight conferred for the observable in analysis. $y_{experimental}$ and $y_{calculated}$ are the experimental and calculated value of each observable, respectively. The weight for the observables is given according to its importance and sensibility to the model.

For reducing the possibilities of divergence, it was used the Levenberg-Marquardt algorithm which is more constrained and robust than other methods.

The mass balances obtained experimentally are the basis for the optimization, where the observables are the yields of the components. However, with the isoparaffins introduction it was necessary to consider the ratio between the isoparaffins and the total of paraffins as observable. This upgrade enables a favorable equilibrium establishment between normal and branched paraffins.

The activation energies were previously chosen in the literature ranges to achieve better results.

5. Results

The implementation of isoparaffins in the model introduced more species, reactions and parameters to optimize. The main differences between the previous version of Petroriser and the model obtained in this work are presented in Table 3.

Table 3 – Characteristics and execution time for the models of 2012 and 2014

Model	2012	2014
Composition	PONA	PIONA
Number of components	45	54
Number of reactions	125	187
Number of reversible reactions	0	9
Number of mass balances[2]	31	43
Number of parameters to optimize	27	41
Total execution time for a single mass balance simulation (s)	4,01	20,98

[1] The paraffins lump that was presented in chapter 4.2 and 4.3 will describe the normal paraffins.

[2] Mass balance is an experimental test performed in the conditions established in chapter 3

Total execution time for an iteration of one parameter optimization for a single mass balance (s)	11,95	126,20

It is important to refer that the execution times presented in Table 3 were obtained in a Intel® Core™ 2 (CPU Intel 2.66 GHz, 4GB RAM) for a tolerance error less than 10^{-3}. As presented above, the processor time taken by the simulator is much higher with the new model. The time for one mass balance simulation, i.e. the solution of a mass balance with the given parameters, increases five times. Consequently, the execution time to optimize one parameter for a single mass balance also increases. With the new model version, the optimization for a given set of parameters and mass balances can take more than 72 h. The longtime required for parameters optimization has restrained the number of modifications that could be implemented in the model and tested.

The high execution time can be justified by the simulator structure. The mass balances are solved in dynamic state and its convergence is obtained when the steady state is achieved. With the introduction of new species and additional reversible reactions it was already expected that the time to reach the steady state would be even longer.

One of the long-term goals in the second riser model development is to obtain a single set of kinetic parameters for all type of feeds. To approach this goal it was first tried to group the feeds. By analyzing their composition (Fig. 1) it seems evident that there are two types of feeds and subsequently two sets of pre-exponential factors. The gasolines are composed by a complex PIONA family and must be concerned in one of these sets. The oligomers are composed mainly by olefins and isoparaffins and are able to be represented in the other set.

After optimizing the parameters, it was possible to conclude that gasolines can be represented by one set of pre-exponential constants, without significantly deteriorating the model quality of prediction. The same method was tried for the oligomers, however for this type of feed the results are worst. This is probably justified for the use of different catalysts in the experimental tests (see Table 1). The catalyst A used in PolyC3C4 tests has a higher content of rare-earth than catalyst B used in PolyC4 tests. Rare-earth content in FCC catalyst is known to promote the catalytic activity, but it also promotes the hydrogen transfer reaction. Furthermore, E-cat A has much higher content of metal contaminants such as nickel and vanadium than E-cat B, and it is well accepted that metals contaminants decrease the catalytic cracking performance. Finally, catalyst B (used in PolyC4 tests) has a higher content in matrix that is supposed to favor the cracking of large molecules and it has also a higher content in ZSM-5. However, without a full characterization of catalysts it is difficult to conclude about their effects in the results.

It has then been decided to keep three different sets of pre-exponential constants: one single set for all gasoline type feeds (catalytic and coker gasoline) and two different sets for the two oligomers respectively.

The structure parameters for linear and branched paraffins also need to be analyzed. It was assumed for both cases the same type of function that takes into account the chain-length and the cracking symmetry. However, different parameters for normal and iso paraffins were estimated to define this function. Fig. 7 presents its results for C_{12} normal- and iso- paraffins cracking situation.

If the C_{12} is a normal paraffin the effect of the structure function it will be close to what is expected, i.e. a smooth normal distribution function (Fig. 2). On the other hand, if the C_{12} is an isoparaffin the consequence is a very abrupt response.

The function presents a very high value for cracking reactions that produce two molecules with 6 carbon atoms (almost 14 times higher than the analogue for linear paraffins), while for a non-symmetric cracking the function response is nearly zero.

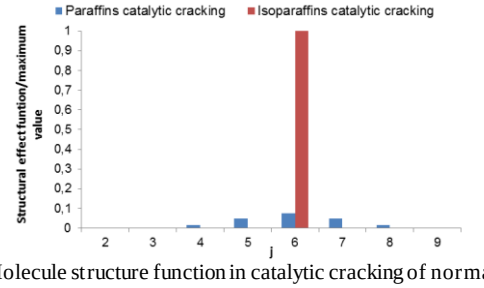

Fig. 7 - Molecule structure function in catalytic cracking of normal and branched paraffins with 12 carbon atoms ($i = 12$). The values were normalized with the maximum value of both situations.

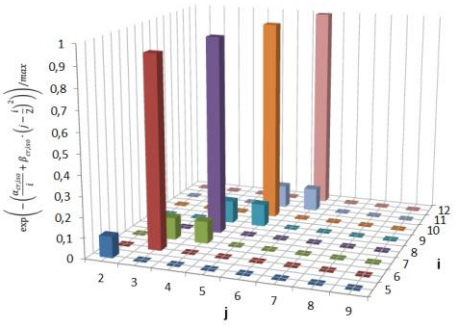

Fig. 8 - Result representation of molecule structure function for isoparaffins catalytic cracking normalized with its maximum value

Fig. 8 represents the isoparaffins results for this function in the applicability range. As discussed above, the function just predicts the effect for the symmetrical cracking cases since for the other cases its value is nearly zero. Besides, the values for this function are much lower (10 times less) for the molecules with odd carbon atoms number. This behavior for isoparaffins is not expected and will affect the results for linear and branched paraffins. In conclusion, the molecule structure function for isoparaffins cracking needs to be reevaluated.

In the next topics, the simulator and experimental results are compared in the form of parity diagrams. Firstly, the FCC main standard cuts will be analyzed and after the lumps that have more relevance in terms of model improvements. This analysis will be done separately for gasoline, PolyC3C4, and PolyC4 and will be related to the results of the previous version dating from 2012.

Standard cuts yields prediction for all the feeds

Firstly, it is useful to analyze the yields prediction of the main cuts of all feeds in the same representation to have an overall idea of the model performance.

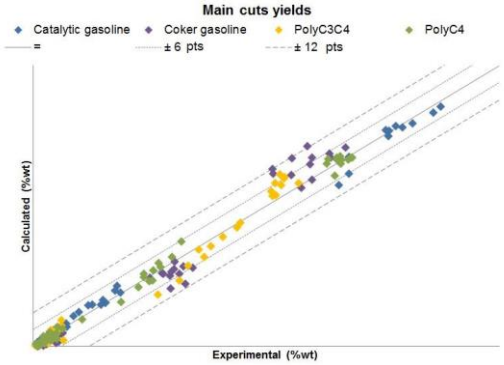

Fig. 9 - Main cuts yields parity diagram for all the feeds

Fig. 9 represents the parity diagram for this situation. This type of charts will be supported by lines that represent the parity axis (denoted as "=") and two tolerance lines (symbolized as

"±X" where X is the value of the absolute error, in points). The tolerance appears as absolute error and is calculated by the difference between the experimental and calculated yield. For the catalytic and coker gasoline predictions, obtained with the same set of parameters, it is clear the difference between their reactivity. Coker gasoline is the feed presenting more dispersion and less accuracy.

Total paraffins

It will be analyzed the total paraffins (the sum between normal and branched) composition in order to compare the results obtained in 2014 and 2012.

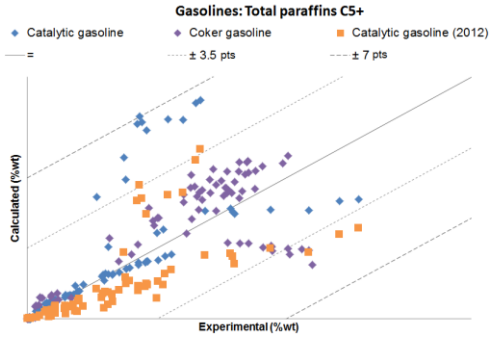

Fig. 10 - Parity diagram of total paraffins lump in gasoline cut for catalytic and coker gasolines

The results for catalytic gasoline are more dispersed with the new model where the margin of tolerance increases from ±3.5 points to ±6.5 points (Fig. 10). The specie that is more overestimated is C_5.

The results of coker gasoline are also dispersed. However, it has an inferior tolerance than catalytic gasoline. In this case, C_5 is the specie that is more underestimated.

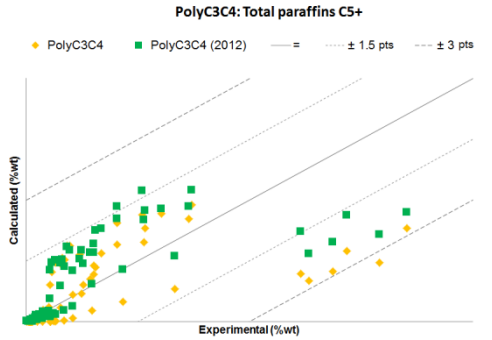

Fig. 11 - Parity diagram of total paraffins lump in gasoline cut for PolyC3C4

According with Fig. 11, PolyC3C4 results are underestimated comparing with the older ones. C_7 is the specie that is more underestimated. Globally, the accuracy decreases for its results.

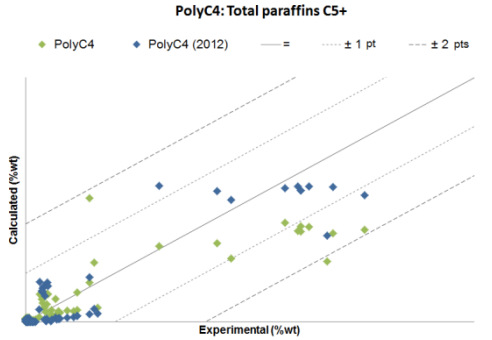

Fig. 12 - Parity diagram of total paraffins lump in gasoline cut for PolyC4

The yields for PolyC4 were obtained with more accuracy for low yields than the previous one, as showed in Fig. 12. However, the results for high yields, that correspond to C_5, decrease the accuracy.

Isoparaffins

The isoparaffins family was introduced in the present work, and for that reason the comparison with the 2012 results is not possible. It will be presented the general results of the family. To understand the quality of the implementation in the next topic the ratio between the branched and total paraffins will be discussed.

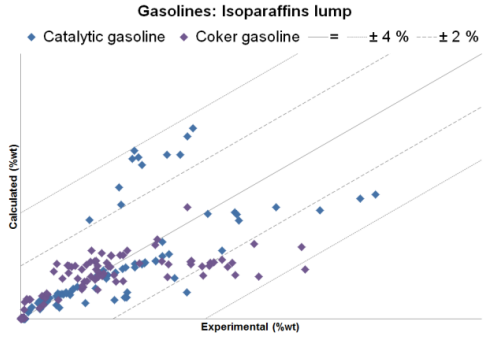

Fig. 13 - Parity diagram of isoparaffins lump (C_4-C_{12}) for catalytic and coker gasoline

Starting with the catalytic gasoline, it is possible to observe that some tests are underestimated and others are overestimated. The results overestimated correspond to iP_5 results and the underestimation to iP_4 and iP_6 results. On the other hand, the results of coker gasoline which are underestimated correspond to iP_4 and iP_5 results.

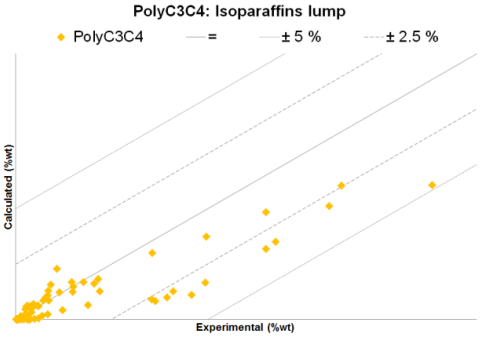

Fig. 14 - Parity diagram of isoparaffins lump (C_4-C_{12}) for PolyC3C4

In the results of PolyC3C4 it is notorious also an underestimation of some points. These points represent the results of iP_4 and iP_7 that are the species with high yields.

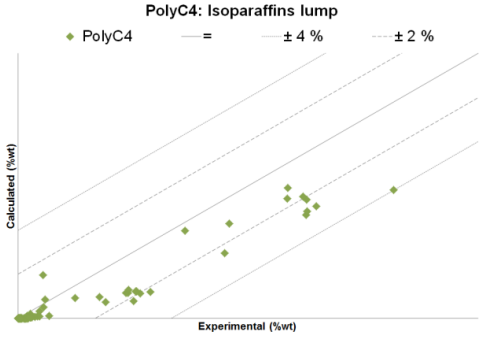

Fig. 15 - Parity diagram of isoparaffins lump (C_4-C_{12}) for PolyC4

A similar deviation is detected for PolyC4, where the underestimation described the iP_4 and iP_5 results.

Ratio isoparaffins/total paraffins

The suitable results of the ratio between isoparaffins and paraffins are achieved with the alteration of objective function[3]. The result analysis will be done component by component, where it will expose the four charges in the same representation.

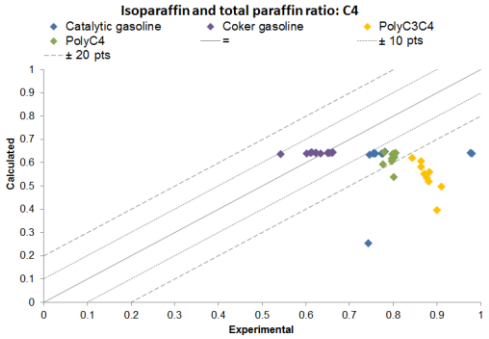

Fig. 16 – Isoparaffin and total paraffin ratio for C_4

Fig. 16 shows that coker gasoline feed is a higher accuracy than the other in the ratio between isoparaffins and normal paraffins. The majority of experimental tests of catalytic gasoline are predicted within a tolerance lower than -15 points. Nevertheless, three of the catalytic gasoline tests are estimated with a much higher deviation (two with a tolerance of -35 points and the other with -50 points). Analyzing these three experimental tests, it was concluded that they were tested with extreme operation condition (higher/lower temperature) than the others. The oligomer feeds results are obtained with a greater tolerance than gasolines (excluding the three points of catalytic gasoline). This result is quite expected, once the oligomers have a weak composition in normal and branched paraffins.

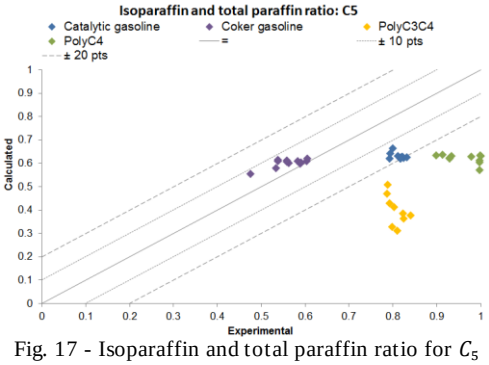

Fig. 17 - Isoparaffin and total paraffin ratio for C_5

The results of ratio between iP_5 and the total paraffins C_5 are presented in Fig. 17. Once again, the ratio is predicted with more exactitude for the gasolines. However, all the tests of catalytic gasoline are predicted with a similar accuracy.

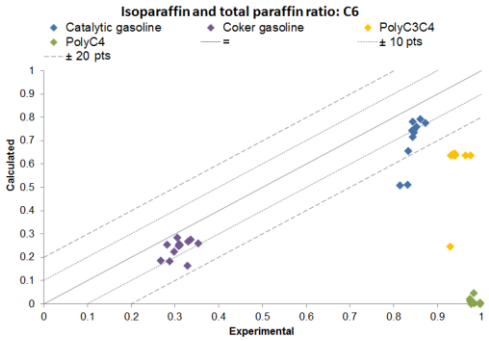

Fig. 18 - Isoparaffin and total paraffin ratio for C_6

The results for C_6, presented in Fig. 18, have the same behavior than C_4: the catalytic gasoline has two points that have a much greater tolerance than the others. These experimental essays were tested with a lower and a higher temperature and higher C/O. The same behavior is observed with PolyC3C4, where the point that has less accuracy it was tested with a higher C/O. Concerning PolyC4, the simulator cannot predict the formation of isoparaffins, where the experimental data indicates the opposite, i.e. the paraffins in output are just branched.

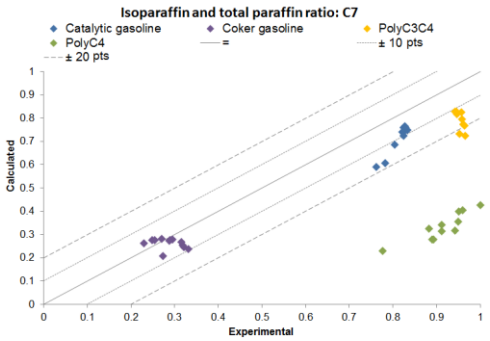

Fig. 19 - Isoparaffin and total paraffin ratio for C_7

The C_7 ratio results are displayed in Fig. 19. By observation of this parity diagram it is perceived that the estimation of equilibrium between normal and branched is not well predicted for PolyC4. An equivalent performance happens with C_8 species where the results appear to have a stochastic behavior.

6. Conclusions

A kinetic model of naphtha catalytic cracking has been developed at IFPEN to be applied in a dual riser configuration. The main development that this work proposes is the distinction between linear and branched paraffins.

The model upgrade from PONA to PIONA introduced more variables and increased the simulator sensitivity. The problems to obtain convergence were more important for the mass balances obtained with more severe conditions, i.e. experimental tests that are obtained with higher/lower temperature and/or C/O than the normal.

Concerning the pre-exponential factor, the gasolines were grouped in the same set to reduce the number of these factors. The same procedure was tried with oligomer feeds without success. The use of different catalysts in the experimental tests can be responsible for the distinct reactivities of these charges.

The molecule structure function was evaluated in order to compare the results between linear and branched paraffins. With the structure parameters that are calculated by the simulator, the function performs the expected effect for normal paraffins, a smooth normal distribution. However, the results for branched paraffins show a very abrupt normal distribution. This distribution predicts a high effect in the symmetric cracking and neglects the other cases. With that, it is possible to conclude that the present function is not suitable to be applied in isoparaffins catalytic cracking. The structure function should be reevaluated.

The results were evaluated by parity diagrams and compared with the previous model. Generally, the cuts' results did not change in a scale worth of consideration. The same can be noticed for the families. Looking to the work focus, the way to compare the new results to the previous ones is by the total paraffins yields. For the catalytic gasoline, the total paraffins yield is obtained with higher dispersion and much overestimation comparing to the 2012 model. The dispersion is also noticed in coker gasoline. Concerning the oligomers, the simulator predicts slight underestimated yields comparing to the 2012 results. The prediction of total paraffins was not improved.

With the results analysis of isoparaffins lump, it was possible to observe that some species are much over/underestimated than others. It is most notorious in gasolines, where iP_5 are overestimated and iP_4 and iP_6 are underestimated in catalytic gasoline results. On the other hand,

[3] Introduction of the ratio between the isoparaffins and the total of paraffins as observable (described in chapter 4.6)

for coker gasoline, the underestimation is related to iP_5 and iP_7. One of the causes for that can be the reaction network proposed. It was assumed that paraffins catalytic cracking do not produce branched paraffins, in order to reduce the number of reactions. However, this assumption is not correct. According to the literature review, the cracking of a linear or a branched paraffin can produced a linear or branched species.

The ratio between the isoparaffins and total paraffins for the same carbon number is important to understand the implementation in terms of equilibrium. As expected the results for this ratio are more accurate for gasolines than for oligomers that can be explained by their composition in paraffins. The results also reveal that the simulator shows also a significant sensitivity to operation. The experimental tests obtained with a lower/higher temperature and/or higher C/O than the typical conditions have worst results and lower accuracy than the others. This sensitivity can be explained by the equilibrium data that are used that cannot be suitable for these severe operating conditions.

The global results did not show an improvement. The isoparaffins implementation was done without deteriorating overmuch the results that is a success for the first approach to introduce the new family. This model is able to achieve good results for each feed for PIONA composition. To improve the results it is necessary to develop the isoparaffins description.

Notation

Symbols

A_x	Aromatic with x carbon atoms
C_x	Hydrocarbon with x carbon atoms
C/O	Cat to oil ratio
Ea	Activation energy ($J\ mol^{-1}$)
G_r	Gibbs free energy ($J\ mol^{-1}$)
H_2O	Water
H_f	Enthalpy of formation ($J\ mol^{-1}$)
iP_x	Isoparaffin with x carbon atoms
K	Rate constant ($Pa\ s^{-1}$)
K^0	Pre-exponential factor ($Pa\ s^{-1}$)
K_{eq}	Equilibrium constant
N_x	Naphthene with x carbon atoms
N_{comp}	Naphetenes group with five or more than six carbon atoms
O_x	Olefin with x carbon atoms
Pp	Partial pressure (Pa)
P_x	Paraffin with x carbon atoms
R	Universal gas constant ($J.mol^{-1}.K^{-1}$)
T	Temperature (K)
S_f	Entropy of formation ($J.mol^{-1}.K^{-1}$)
y_{LCO}	Number of hydrogen atoms considered for LCO
y_{Coke}	Number of hydrogen atoms considered for coke
x_{LCO}	Number of carbon atoms considered for LCO
x_{Coke}	Number of carbon atoms considered for coke
Z/M	Zeolite to matrix ratio

Greek letters

α	dependence factor on the reactant's carbon number, a.u.
β	symmetry governing factor, affecting product distribution, a.u.

Subscripts, Superscripts and Abbreviations

Cycli	Cyclization
E-cat	Equilibrium catalyst
FCC	Fluid Catalytic Cracking
HCN	Heavy cracked naphtha
HCO	Heavy cycle oil
ht1	Step 1 of hydrogen transfer
ht2	Step 2 of hydrogen transfer
ht3	Step 3 of hydrogen transfer
Iso	Isoparaffin
Isom	Isomerization
LCN	Light cracked naphtha
LCO	Light cycle oil
LPG	Liquefied petroleum gases
Ocr	Olefins catalytic cracking
Oligom	Oligomerization
Pcr	Paraffins catalytic cracking
Ref	reference
REO	Rare-earth oxides
th1	Olefins thermal cracking
th2	Paraffins thermal cracking

References

[1] A. J. Nizamoff, "Propylene PERP 2013-1," Nexant, New York, 2013.

[2] V. Y. Wan, "Propylene production bt the JGC/MMC DTP process," IHS, Santa Clara, 2012.

[3] M. P. Do, Writer, *FCC – Flexible Responses to Market's Evolution*. [Performance]. Axens, 2009.

[4] Concawe, "Oil refining in the EU in 2020, with perspectives to 2030," Concawe, Brussels, 2013.

[5] F. Feugnet and R. Roux, "Process for catalytic cracking with a recycle of an olefinic cut removed upstream of the gas separation section in order to maximize propylene production". US Patent 0272326A1, 2011.

[6] N. Rahimi and R. Karimzadeh, "Catalytic cracking of hydrocarbons over modified ZSM-5 zeolites to produce light olefins: A review," *Applied Catalysis*, vol. General, no. 398, pp. 1-17, 2011.

[7] F. Feugnet, "Naphtha cracking modelling," IFP Energies Nouvelles, Lyon, 2008.

[8] J. Fernandes, "Naphtha cracking modeling : New fit for HPFCC application," IFP Energies nouvelles, Lyon, 2010.

[9] A. Palma, Kinetic Model for Gasoline Catalytic Cracking Based on a Lumped Molecular Approach, Lisboa: Técnico Lisboa, 2012.

[10] L. Wang, B. Yang and Z. Wang, "Lumps and kinetics for the secondary reactions in catalytically cracked gasoline," *Chemical Engineering Journal*, vol. 109, pp. 1-9, 2005.

[11] C. Pinheiro, F. Lemos and F. Râmoa Ribeiro, "Dynamic modelling and network simulation of n-heptane catalytic cracking: influence of kinetic parameters," *Chemical Engeneering Science*, pp. 1735-1750, 1999.

[12] H. Carabineiro, C. Pinheiro, F. Lemos and F. Ribeiro, "Transient microkinetic modelling of n-heptane catalytic cracking over H-USY zeolite," *Chemical Engineering Science*, pp. 1221-1232, 2003.

[13] J. Joly, J. Vleeming and P. Galtier, "Isomerization of n-butane and isobutane with IS612A as catalyst. Results of the kinetic experiments," Institut Français du Pétrole, Lyon, 1997.